

Geometric Complementarity in Assembly and Guest Recognition of a Bent Heteroleptic cis-[Pd₂LA₂LB₂] Coordination Cage

Witold Marek Bloch, Yoko Abe, Julian Jakob Holstein,
Claudia M. Wandtke, Birger Dittrich, and Guido H. Clever

J. Am. Chem. Soc., **Just Accepted Manuscript** • DOI: 10.1021/jacs.6b08694 • Publication Date (Web): 22 Sep 2016

Downloaded from <http://pubs.acs.org> on September 22, 2016

Just Accepted

“Just Accepted” manuscripts have been peer-reviewed and accepted for publication. They are posted online prior to technical editing, formatting for publication and author proofing. The American Chemical Society provides “Just Accepted” as a free service to the research community to expedite the dissemination of scientific material as soon as possible after acceptance. “Just Accepted” manuscripts appear in full in PDF format accompanied by an HTML abstract. “Just Accepted” manuscripts have been fully peer reviewed, but should not be considered the official version of record. They are accessible to all readers and citable by the Digital Object Identifier (DOI®). “Just Accepted” is an optional service offered to authors. Therefore, the “Just Accepted” Web site may not include all articles that will be published in the journal. After a manuscript is technically edited and formatted, it will be removed from the “Just Accepted” Web site and published as an ASAP article. Note that technical editing may introduce minor changes to the manuscript text and/or graphics which could affect content, and all legal disclaimers and ethical guidelines that apply to the journal pertain. ACS cannot be held responsible for errors or consequences arising from the use of information contained in these “Just Accepted” manuscripts.

Geometric Complementarity in Assembly and Guest Recognition of a Bent Heteroleptic cis -[Pd₂L^A₂L^B₂] Coordination Cage

Witold M. Bloch,[†] Yoko Abe,[†] Julian J. Holstein,[†] Claudia M. Wandtke,[§] Birger Dittrich,[‡] Guido H. Clever^{*,†}

[†] Faculty of Chemistry and Chemical Biology, TU Dortmund University, Otto-Hahn-Straße 6, 44227 Dortmund (Germany).

[§] Institute for Inorganic Chemistry, Georg-August University Göttingen, Tammannstraße 4, 37077 Göttingen (Germany).

[‡] Institute for Inorganic Chemistry and Structural Chemistry, Heinrich-Heine University Düsseldorf, Universitätsstraße 1, 40225 Düsseldorf (Germany).

ABSTRACT: Due to the inherent difficulties in achieving a defined and exclusive formation of multi-component assemblies against entropic predisposition, we present the rational assembly of a heteroleptic [Pd₂L^A₂L^B₂]⁴⁺ coordination cage achieved through the geometric complementarity of two carefully designed ligands, L^A and L^B. With Pd(II) cations as rigid nodes, the pure distinctly angular components readily form homoleptic cages; a [Pd₂L^A₄]⁴⁺ strained helical assembly and a [Pd₄L^B₈]⁸⁺ box-like structure, both of which were characterized by X-ray analysis. Combined however, the two ligands could be used to cleanly assemble a cis -[Pd₂L^A₂L^B₂]⁴⁺ cage with a bent architecture. The same self-sorted product was also obtained by a quantitative cage-to-cage transformation upon mixing of the two homoleptic cages revealing the [Pd₂L^A₂L^B₂]⁴⁺ assembly as the thermodynamic minimum. The structure of the heteroleptic cage was examined by ESI-MS, COSY, DOSY and NOESY methods, the latter of which pointed towards a cis -conformation of ligands in the assembly. Indeed, DFT calculations revealed the angular ligands and strict Pd(II) geometry strongly favor the cis -[Pd₂L^A₂L^B₂]⁴⁺ species. The robust nature of the cis -[Pd₂L^A₂L^B₂]⁴⁺ cage allowed us to probe the accessibility of its cavity, which could be utilized for shape recognition towards stereoisomeric guests. The ability to directly combine two different backbones in a controlled manner provides a powerful strategy for increasing complexity in the family of [Pd₂L₄] cages and opens up possibilities of introducing multiple functionalities into a single self-assembled architecture.

INTRODUCTION

Inspired by the function and complexity of biological systems, the design of artificial supramolecular host assemblies has become a burgeoning area of study, particularly utilizing the powerful tool of coordination-driven self-assembly from ligand and metal building blocks.¹ The adjustable cavity of resulting assemblies has produced host systems capable of acting as chemical sensors,² drug transporters,³ components of complex systems,⁴ stabilization media⁵ and more.^{1c,6} Much of this however, has been achieved by relatively simple homoleptic assemblies consisting of one type of ligand. For the purpose of approaching greater complexity and functionality, the derivation of strategies to control the arrangement of different ligand entities in a single assembly is an area which has recently received much attention.⁷ For example, Zheng and Stang's charge separation,⁷ⁿ Schmittel's steric constraints^{7s} and Fujita's side chain-directed approach^{7r} are among some of the proven methods to access both complex and functional heteroleptic metallosupramolecular architectures.⁸

[M₂L₄] coordination cages assembled from square-planar metal cations such as Pd(II), Pt(II), Cu(II) and

Ni(II) and banana-shaped bis-monodentate ligands are a family of robust and diverse molecular hosts with the ability to provide accessible cavities due to their symmetric and spatial arrangement of ligands.⁹ The properties of the most intensively studied [Pd₂L₄] cages are often imparted through functionalization of the ligand components, a strategy which has yielded assemblies with attractive properties such as selective guest binding,^{3c,10} stimuli responsive structural transitions,¹¹ or rearrangements,¹² redox properties,¹³ and biological activity.¹⁴ However, there still remains great scope to extend the complexity and functionality of these architecturally simple assemblies by incorporating more than one type of ligand entity into the structure. Controlled formation of heteroleptic [Pd₂L₂L'₂]⁴⁺ assemblies from unprotected Pd(II) cations however has seldom been reported; often the combination of a metal ion with two or more distinct ligands leads to uncontrolled statistical mixtures or narcissistic self sorting,¹⁵ especially in the case of N-donor coordinated Pd(II).¹⁶ Nevertheless, some examples exist: Hooley and co-workers reported a degree of control over the formation of heteroleptic cages by endohedral functionalization of banana-shaped ligands with differing

degrees of steric bulk. A 1:1 mixture of a $[\text{Pd}_2\text{L}_4]^{4+}$ and $[\text{Pd}_2\text{L}_2\text{L}'_2]^{4+}$ species could be observed with a combination of bulky and non-bulky ligands.¹⁷ On the other hand, Yoshizawa recently reported a $[\text{Pd}_2\text{L}_2\text{L}'_2]^{4+}$ cage achieved through a template effect with a C60 guest.¹⁸ While these systems nicely showcase different strategies to achieve heteroleptic assemblies, they suffer from the problem that their formation is inevitably linked to an already occupied cavity.

Most recently, Crowley and co-workers reported a strategy to achieve controlled formation of $[\text{Pd}_2\text{L}_2\text{L}'_2]^{4+}$ coordination cages through exploitation of H-bonding between electron-rich 2-amino substituted pyridyl ligand components.¹⁹ Intriguingly, the kinetically driven heteroleptic assembly could only be accessed through ligand displacement reactions, rather than from direct ligand assembly or cage-to-cage conversion of their homoleptic counterparts. Apart from these examples, strategies to access coordinatively saturated Pd(II) cage assemblies from at least two distinct ligand components remain scarce.

Herein we report the pre-programming of ligand components (L^{A} and L^{B}) with shape complementarity based on a directional bonding approach²⁰ as a robust route to the controlled and template-free formation of a 3-component $[\text{Pd}_2\text{L}^{\text{A}}_2\text{L}^{\text{B}}_2]^{4+}$ assembly (C_3). In contrast with most previously reported multi-component assembly strategies,⁷ the formation here does not rely upon the combination of different donor sets or implementation of steric bulk, but rather the energy benefit associated with utilizing ligands of a complementary shape, which results in the heteroleptic assembly as the stable, thermodynamic product.

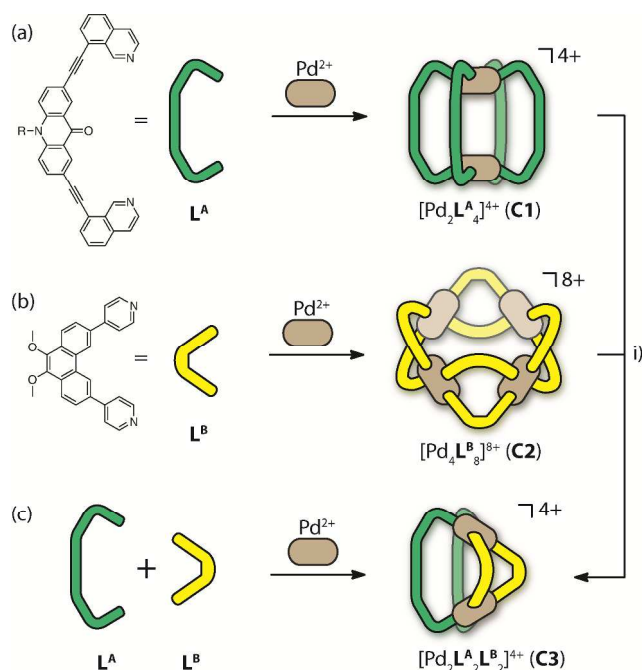


Figure 1. Self-assembly scheme showing the ligands and coordination cages presented in this work; a) self-assembly of a

homoleptic $[\text{Pd}_2\text{L}^{\text{A}}_4]^{4+}$ cage (C_1); b) self-assembly of a homoleptic $[\text{Pd}_4\text{L}^{\text{B}}_8]^{8+}$ box (C_2); c) three-component self-assembly of a heteroleptic $[\text{Pd}_2\text{L}^{\text{A}}_2\text{L}^{\text{B}}_2]^{4+}$ cage (C_3), achieved either from the individual ligand components and Pd(II) or by (i) mixing C_1 and C_2 in a 2:1 ratio.

RESULTS AND DISCUSSION

Synthesis of ligands L^{A} and L^{B} . Initially, we compared the formation of homo- and heteroleptic self-assemblies based on the two shape complementary ligands L^{A} and L^{B} (Figure 1). Therefore, ligand L^{A} was synthesized by Sonogashira cross-coupling of 2,7-dibromo-10-hexylacridin-9(10H)-one with 8-ethynyl-isoquinoline, whilst ligand L^{B} was prepared by a Suzuki coupling of 3,6-dibromo-9,10-dimethoxyphenanthrene and 4-pyridineboronic acid pinacol ester. The structures of L^{A} and L^{B} were confirmed using NMR spectroscopy, mass spectrometry, and X-ray crystallography (Supporting Information). We then turned our attention to investigating the respective Pd-mediated homoleptic assemblies of L^{A} and L^{B} .

Homoleptic assembly of cages C_1 and C_2 . With regards to L^{A} , we anticipated that the eight inward-pointing isoquinoline donors may have to undergo severe twisting in a $[\text{Pd}_2\text{L}^{\text{A}}_4]^{4+}$ assembly. Heating a 2:1 mixture of L^{A} and $[\text{Pd}(\text{CH}_3\text{CN})_4](\text{BF}_4)_2$ in DMSO at 70 °C for 2 h resulted in the quantitative formation of a single product, identified as a $[\text{Pd}_2\text{L}^{\text{A}}_4]^{4+}$ cage (C_1) by ^1H NMR spectroscopy (Figure 2b) and mass spectrometry (Figure S27). The ^1H NMR spectrum of C_1 revealed a significant upfield shift of several isoquinoline and acridone proton signals of L^{A} (Figure 2a and b), suggesting shielding by a neighboring π -system due to twisting and dense association of the ligand backbones. Indeed the X-ray structure of C_1 revealed that the four ligands (two of which are crystallographically unique) are in a highly twisted conformation, participating in either π -stacking or hydrogen bonding with neighboring backbones, resulting in a helical assembly (Figure 5a). Due to packing effects, C_1 contains C_2 symmetry in the solid-state, however the number of observed NMR signals indicates that the overall flexibility of the assembly allows for a higher, fourfold symmetry in solution. Noteworthy is the compressed nature of the structure, with a Pd...Pd distance of 15.05 Å.

For the Pd-mediated assembly of L^{B} , we expected a different structure due to the para-substituted pyridine donors which create an approximate 60° vector angle with respect to the phenanthrene backbone. Indeed, heating a 2:1 mixture of L^{B} and $[\text{Pd}(\text{CH}_3\text{CN})_4](\text{BF}_4)_2$ in DMSO at 70 °C for 2 h resulted in the quantitative formation of a $[\text{Pd}_4\text{L}^{\text{B}}_8]^{8+}$ (C_2) cage species (Figure 1b). The ESI HR-MS spectrum was consistent with only one major species, yielding signals for ions of $[\text{Pd}_4\text{L}^{\text{B}}_8+n\text{BF}_4]^{8-n+}$ ($n=1-4$) (Figure S28). In the ^1H NMR spectrum, downfield shifts of pyridyl protons H_e and H_d were observed (Figure 2e,d), consistent with Pd(II) complexation. Along with 2D NMR analysis, these observations pointed towards a D_{4h} symmetric M_4L_8 'box' structure for C_2 , a topology that has previously been encountered by Fujita and co-workers

using a similar ligand.²¹ The structure of **C2** was confirmed by X-ray crystallography which revealed the expected connectivity (Figure 5b). Due to packing effects the assembly deviates slightly from ideal D_{4h} symmetry, with the opposing Pd...Pd distances measuring 17.44 and 16.73 Å respectively.

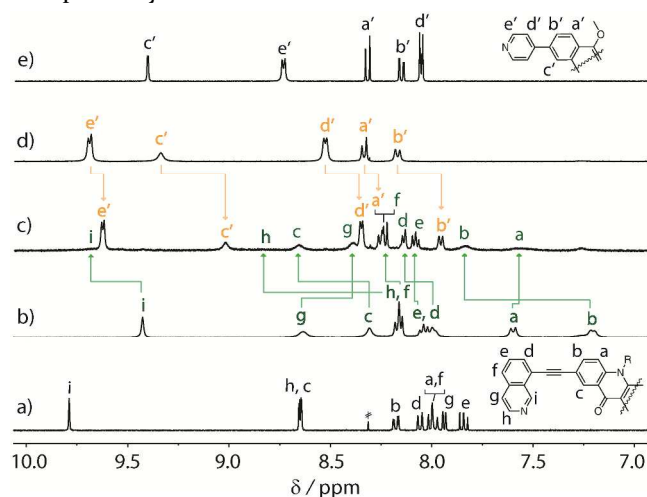


Figure 2. Partial ^1H NMR (400 MHz/DMSO- d_6 , 25°C) spectra showing the self-assembly of $[\text{Pd}_2\text{L}_4]^{4+}$ (**C1**), $[\text{Pd}_4\text{L}_8]^{8+}$ (**C2**), and $[\text{Pd}_2\text{L}_2^{\text{A}}\text{L}_2^{\text{B}}]^{4+}$ (**C3**); a) L^{A} ; b) $[\text{Pd}_2\text{L}_4]^{4+}$ obtained by heating L^{A} with 0.5 equiv of Pd(II); c) $[\text{Pd}_2\text{L}_2^{\text{A}}\text{L}_2^{\text{B}}]^{4+}$ obtained by heating a 1:1:1 mixture of L^{A} , L^{B} and Pd(II), or a 2:1 mixture of $[\text{Pd}_2\text{L}_4]^{4+}$ and $[\text{Pd}_4\text{L}_8]^{8+}$, respectively; d) $[\text{Pd}_4\text{L}_8]^{8+}$ obtained from heating L^{B} and 0.5 equiv of Pd(II); e) L^{B} .

Heteroleptic assembly of cage C3. For the target $[\text{Pd}_2\text{L}_2^{\text{A}}\text{L}_2^{\text{B}}]^{4+}$ heteroleptic assembly, molecular modeling suggested that the geometric constraints imposed by the metal and ligand components should behave synergistically to yield only one cage isomer. DFT calculations indicated that compared to the *trans*- $[\text{Pd}_2\text{L}_2^{\text{A}}\text{L}_2^{\text{B}}]^{4+}$ cage (+131.8 kJ/mol) the formation of the *cis*- $[\text{Pd}_2\text{L}_2^{\text{A}}\text{L}_2^{\text{B}}]^{4+}$ cage from its components is significantly more energetically favorable (-65.6 kJ/mol) due to the complementary arrangement of the ligands with respect to the Pd(II) coordination sphere. In addition, cages obeying the stoichiometries $[\text{Pd}_2\text{L}_3^{\text{A}}\text{L}_1^{\text{B}}]^{4+}$ and $[\text{Pd}_2\text{L}_1^{\text{A}}\text{L}_3^{\text{B}}]^{4+}$ were found to be higher in energy than the *cis*-isomer (Figure 3). Therefore we expected that the square planar geometry of Pd(II) and the respective backbone angles of L^{A} and L^{B} should strongly favor a *cis* arrangement of the ligands.

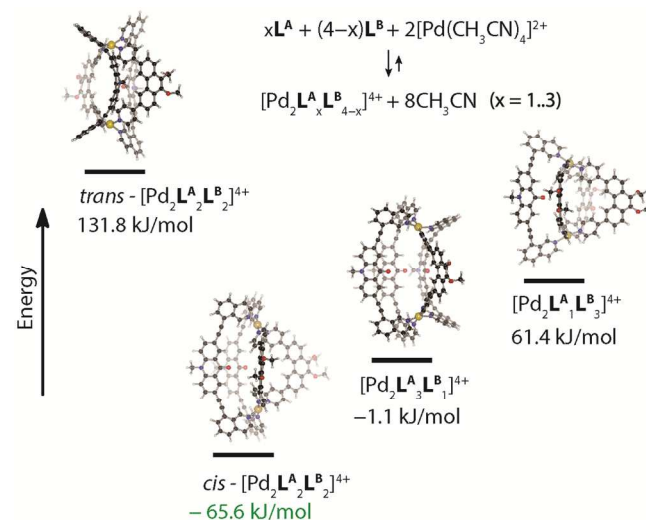


Figure 3. Energy diagram with DFT calculated structures of *trans*- $[\text{Pd}_2\text{L}_2^{\text{A}}\text{L}_2^{\text{B}}]^{4+}$, *cis*- $[\text{Pd}_2\text{L}_2^{\text{A}}\text{L}_2^{\text{B}}]^{4+}$, $[\text{Pd}_2\text{L}_3^{\text{A}}\text{L}_1^{\text{B}}]^{4+}$ and $[\text{Pd}_2\text{L}_1^{\text{A}}\text{L}_3^{\text{B}}]^{4+}$. The energies of the respective cages were calculated according to equations described in the supporting information. To simplify the calculations, the hexyl chain of the acridone moiety of L^{A} was replaced with a methyl substituent.

Indeed, heating a mixture of L^{A} , L^{B} and $[\text{Pd}(\text{CH}_3\text{CN})_4](\text{BF}_4)_2$ in a 1:1:1 ratio for 2 h at 70 °C gave rise to a single species with a distinct ^1H NMR spectrum (Figure 2c). Interestingly, the isoquinoline protons of L^{A} , H_i and H_h , were significantly broadened in the room temperature NMR spectra. Therefore, we performed variable temperature ^1H NMR experiments (Figure S16) which revealed a gradual sharpening of all signals including the isoquinoline protons. We then performed a ^1H - ^1H COSY experiment at 70 °C which allowed complete assignment of the expected set of 14 aromatic proton signals for the heteroleptic $[\text{Pd}_2\text{L}_2^{\text{A}}\text{L}_2^{\text{B}}]^{4+}$ (**C3**) species (Figure S18).

In addition, we performed a NOESY experiment at 70 °C in order to assign the important inter-ligand contacts in **C3** (Figure 4b, Figure S19). Analysis revealed several evident cross-peaks, particularly between the isoquinoline and acridone protons of L^{A} and the pyridyl protons of L^{B} . Importantly, the observed contacts were in full agreement with the calculated model. DOSY analysis confirmed that all of the proton signals assigned to **C3** correspond to the same diffusion coefficient (Figure 4c). Further characterization of the sample by ESI HR-MS yielded a relatively simple spectrum, with the prominent signals assigned to the $[\text{Pd}_2\text{L}_2^{\text{A}}\text{L}_2^{\text{B}} + n\text{BF}_4]^{4-n+}$ species ($n = 0, 1$) (Figure 4a).

Cage-to-cage transformation of C1 and C2 to give C3. Given the rapid and facile assembly of **C3** from L^{A} , L^{B} and Pd(II), we next performed experiments to investigate whether **C3** is the thermodynamic minimum of a mixture of **C1** and **C2**. In contrast to the assembly from the individual ligands, mixing **C1** and **C2** in a 2:1 ratio resulted in a rather slow conversion to the heteroleptic species **C3**, complete after 12 days of heating at 70 °C (Figure S20), presumably due to the requirement of disassembling

multiple coordination bonds.²² We also investigated the conversion to **C**₃ by addition of the either **L**^A or **L**^B to **C**₂ or **C**₁, respectively. We observed that upon addition of **L**^B to **C**₁, **C**₃ was formed immediately at room temperature (Figure S21). Conversely, upon addition of **L**^A to **C**₂, the system reached equilibrium after 2 days of heating at 70 °C with only 10% of **C**₃ formed (Figure S22). We assume differing strain within these species to be responsible for this effect. For the helical structure of **C**₁, addition of **L**^B provides an opportunity to release strain via disassembly and reassembly to **C**₃, whilst the same energy benefit is presumably not provided for the less strained structure of **C**₂.

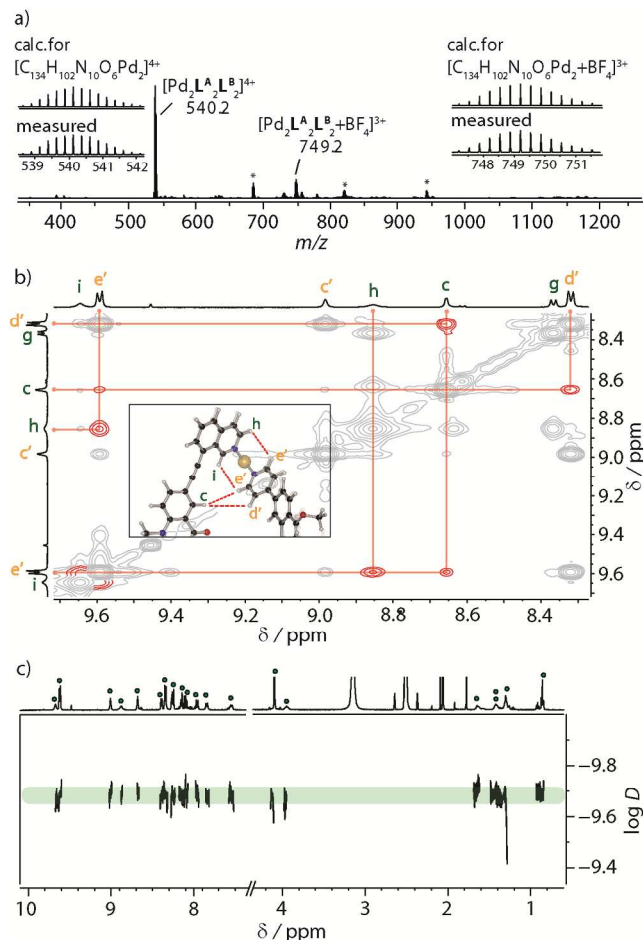


Figure 4. a) ESI mass spectrum of $[\text{Pd}_2\text{L}_2^{\text{A}}\text{L}_2^{\text{B}}+n\text{BF}_4]^{4-n+}$ with $n = 0, 1$ ($* = [\text{Pd}_2\text{L}_3^{\text{A}}\text{L}_2^{\text{B}}+n\text{BF}_4]^{4-n+}$, with $n = 0-2$). b) An expansion of the $^1\text{H} - ^1\text{H}$ NOESY spectrum of **C**₃ measured at 70 °C. The inter-ligand cross peaks are highlighted in red and indicated on the DFT model of **C**₃ in the inset. c) DOSY spectrum (500 MHz/DMSO, 70°C) of **C**₃. All of the signals assigned to **C**₃ (marked with a circle) correspond to the same diffusion coefficient ($2.14 \times 10^{-10} \text{ m}^2 \text{ s}^{-1}$, $\log D = -9.67$).

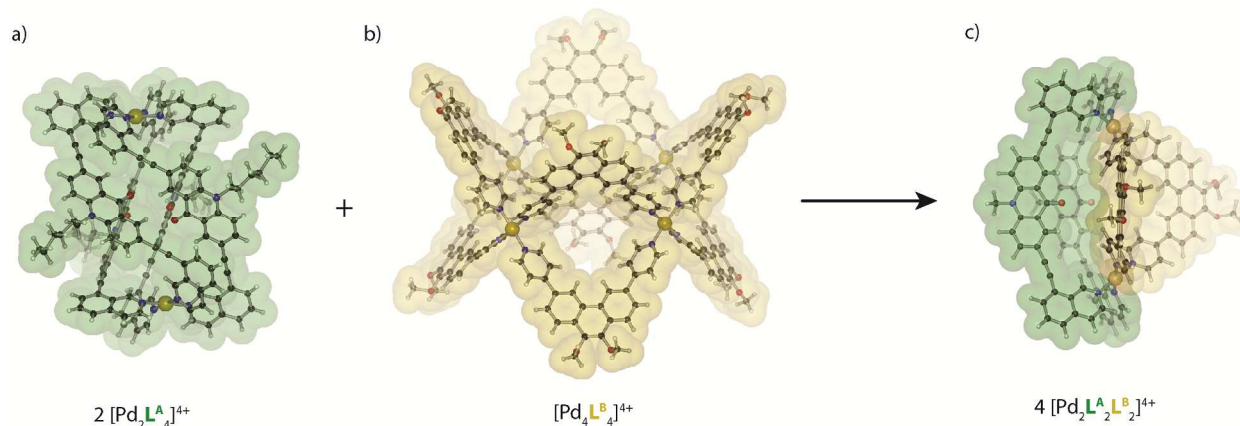


Figure 5. A perspective view of the X-ray crystal structures of a) **C**₁ and b) **C**₂ with counter-ions removed for clarity. c) DFT calculated model of **C**₃. The hexyl chain of **C**₃ was omitted to simplify calculations. The space filling representation is overlaid for each structure (supplementary crystallographic data is found in the Supporting Information and CCDC data sets 1472456, 1489224-1489226). The molar ratios of **C**₁ – **C**₃ associated with the cage-to-cage transformation are included below each struc-

ture. The associated energy benefit as roughly estimated by DFT calculations is discussed in the Supporting Information (Figure SI 31).

Despite numerous attempts, we were not able to obtain single crystals of **C3** suitable for X-ray analysis. To obtain further insight into the assembly of **C3** and investigate the observed intramolecular self-sorting, we further compared the DFT structures of **C1**, **C2**, and **C3** (Figures S31 and 5c) revealing that the cage-to-cage transformation of **C1** and **C2** to **C3** should be highly energetically favored (Figure 5 and the SI) This result supports **C3** as the thermodynamic minimum of the system.

Shape complementary guest binding. It is interesting to note that **C3** is the first example of a $[\text{Pd}_2\text{L}_4]$ coordination cage with a bent architecture. As the Pd(II) metal centers can serve as anchors for charged molecules,²¹ we identified that such host architecture may possess a shape specific cavity for guest binding. To test this hypothesis, we performed ^1H NMR titrations with a straight and bent-shaped guest; 2,7-naphthalene disulfonate (G^1) and the 2,6 analogue (G^2). In both cases, fast exchange was observed relative to the time scale of the experiment (Figure S23 and S24). We determined the host to guest stoichiometry to be 1:1 by the Job plot method (Figure S26), and further verified this by mass spectrometry (Figure S29 and S30). Furthermore, contacts observed in the NOESY analysis of $\text{G}^1@C_3$ (Figure S25) revealed that the disulfonate guest is situated between the acridone backbones of the two adjacent L^A ligands in **C3**, most likely stabilized by π - stacking. Therefore, from the ^1H NMR titrations (Figure 6a) we calculated the association constant between G^1 and **C3** and G^2 and **C3** to be approximately 5200 and 2300 M^{-1} respectively. This difference can be explained by the shape-complementary fit of G^1 relative to the cavity and angular Pd(II) anchors of **C3**. To support these observations, we calculated the structures of $\text{G}^1@C_3$ and $\text{G}^2@C_3$ (Figure 6b and c). A comparison of the minimized energies revealed that $\text{G}^1@C_3$ is stabilized by 40.7 kJ/mol as compared to isomeric complex $\text{G}^2@C_3$, which is in accordance with the optimal fit of G^1 inside the shape-specific cavity of **C3**. Interestingly, previous binding studies of G^1 and G^2 in a $[\text{Pd}_2\text{L}_4]^{4+}$ cage²³ with relationally parallel Pd(II) planes showed a stronger binding for G^2 . Thus, the unusual cavity and angular Pd(II) anchors of **C3** create a shape-specific environment with opposite guest binding preference than the previously studied example.

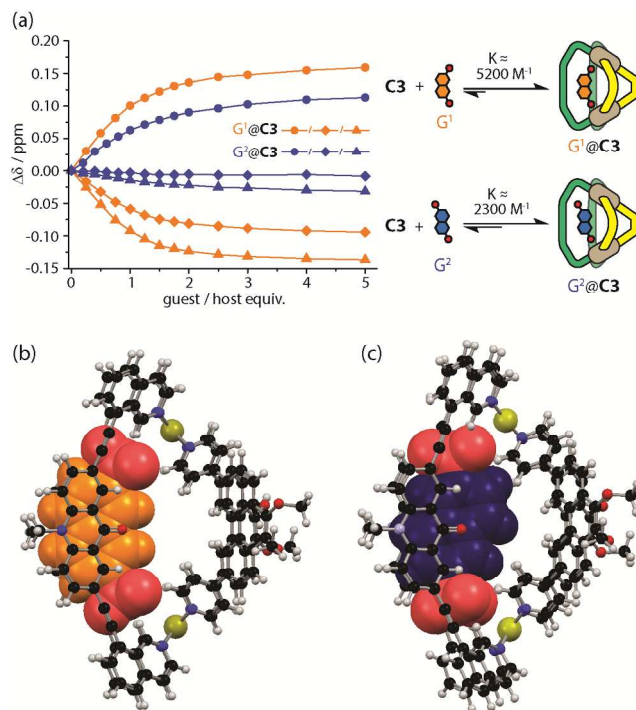


Figure 6. ^1H NMR titrations of **C3** with G^1 and G^2 . Circles, diamonds, and triangles represent the shift of protons H_e , H_c (L^B) and H_c (L^A) respectively. c) and d) show the energy minimized structure of $\text{G}^1@C_3$ and $\text{G}^2@C_3$ respectively.

CONCLUSIONS

In conclusion, we have presented the self-assembly of two complementary ligands L^A and L^B in homoleptic and heteroleptic Pd-mediated coordination cages. We have shown that geometric complementarily pre-programmed into ligand components is a robust strategy to achieve a stable heteroleptic $\text{cis-}[\text{Pd}_2\text{L}^A_2\text{L}^B_2]^{4+}$ cage, thus surmounting the entropic tendency to form a mixture of products. Furthermore, we demonstrated that the heteroleptic architecture can be accessed through multiple self-assembly pathways: direct combination of the ligands with Pd(II), cage-to-cage transformations, and ligand induced cage rearrangements. The latter was found to proceed smoothly only in the case of addition of L^B to **C1**, revealing the possible strain in the **C1** helical species as the driving force for this reaction. The cage-to-cage transformations also highlighted an important feature of our system; the thermodynamic stability of the heteroleptic product, allowing us to probe the cavity of **C3**. The unique shape of **C3** and angular Pd(II) anchors indeed provided an accessible cavity which we exploited in the shape recognition on the level of host-guest binding. We think that the implementation of this strategy into the area of $[\text{Pd}_2\text{L}_4]$ cages may yield new and unique host systems with a greater control over the incorporation of multiple functionalities and hence fine tuning of the chemistry of the cavity. Current investigations into functionalizing the

individual backbones with complementary entities (e.g. electron-donor acceptor system) are underway in our laboratory.

ASSOCIATED CONTENT

Supporting Information. Experimental details and further X-ray, NMR, MS and computational data are presented. This material is available free of charge via the Internet at <http://pubs.acs.org>.

AUTHOR INFORMATION

Corresponding Author

* E-mail: guido.clever@tu-dortmund.de

Notes

The authors declare no competing financial interest

ACKNOWLEDGMENT

We thank Dr. H. Frauendorf (Göttingen) for measuring the ESI mass spectra and Dr. M. John (Gö.) and Prof. Dr. W. Hiller (TU Dortmund) for assistance with NMR measurements and helpful discussions. W.M.B thanks the Alexander von Humboldt Foundation for a postdoctoral fellowship. Y.A. thanks the Japan Society for the Promotion of Science for a fellowship. The Fonds der Chemischen Industrie and the Deutsche Forschungsgemeinschaft (CL 489/2-1) kindly provided financial support. We thank the European Research Council for supporting our further studies in this direction by ERC Consolidator grant 683083 (RAMSES).

REFERENCES

1. a) Fujita, M.; Tominaga, M.; Hori, A.; Therrien, B. *Acc. Chem. Res.* **2005**, *38*, 369; b) Northrop, B. H.; Zheng, Y.-R.; Chi, K.-W.; Stang, P. J. *Acc. Chem. Res.* **2009**, *42*, 1554; c) Chakrabarty, R.; Mukherjee, P. S.; Stang, P. J. *Chem. Rev.* **2011**, *111*, 6810; d) Smulders, M. M. J.; Riddell, I. A.; Browne, C.; Nitschke, J. R. *Chem. Soc. Rev.* **2013**, *42*, 1728; e) Hof, F.; Craig, S. L.; Nuckolls, C.; Rebek, J. J. *Angew. Chem. Int. Ed.* **2002**, *41*, 1488.
2. a) Ahmad, H.; Hazel, B. W.; Meijer, A. J. H. M.; Thomas, J. A.; Wilkinson, K. A. *Chem. Eur. J.* **2013**, *19*, 5081; b) Neelakandan, P. P.; Jimenez, A.; Nitschke, J. R. *Chem. Sci.* **2014**, *5*, 908.
3. a) Therrien, B.; Süß-Fink, G.; Govindaswamy, P.; Renfrew, A. K.; Dyson, P. J. *Angew. Chem. Int. Ed.* **2008**, *47*, 3773; b) Lewis, J. E. M.; Gavey, E. L.; Cameron, S. A.; Crowley, J. D. *Chem. Sci.* **2012**, *3*, 778.
4. a) Inokuma, Y.; Kawano, M.; Fujita, M. *Nat Chem* **2011**, *3*, 349; b) Zarra, S.; Wood, D. M.; Roberts, D. A.; Nitschke, J. R. *Chem. Soc. Rev.* **2015**, *44*, 419.
5. a) Kawano, M.; Kobayashi, Y.; Ozeki, T.; Fujita, M. *J. Am. Chem. Soc.* **2006**, *128*, 6558; b) Fiedler, D.; Bergman, R. G.; Raymond, K. N. *Angew. Chem. Int. Ed.* **2006**, *45*, 745; c) Mal, P.; Breiner, B.; Rissanen, K.; Nitschke, J. R. *Science* **2009**, *324*, 1697.
6. a) Ward, M. D.; Raithby, P. R. *Chem. Soc. Rev.* **2013**, *42*, 1619; b) Cook, T. R.; Stang, P. J. *Chem. Rev.* **2015**, *115*, 7001; c) McConnell, A. J.; Wood, C. S.; Neelakandan, P. P.; Nitschke, J. R. *Chem. Rev.* **2015**, *115*, 7729; d) Brown, C. J.; Toste, F. D.; Bergman, R. G.; Raymond, K. N. *Chem. Rev.* **2015**, *115*, 3012.
7. Reviews: a) De, S.; Mahata, K.; Schmittel, M. *Chem. Soc. Rev.* **2010**, *39*, 1555; b) Saha, M. L.; De, S.; Pramanik, S.; Schmittel, M. *Chem. Soc. Rev.* **2013**, *42*, 6860; c) Mukherjee, S.; Mukherjee, P. S. *Chem. Commun.* **2014**, *50*, 2239; d) Li, H.; Yao, Z.-J.; Liu, D.; Jin, G.-X. *Coord. Chem. Rev.* **2015**, *293-294*, 139; e) He, Z.; Jiang, W.; Schalley, C. A. *Chem. Soc. Rev.* **2015**, *44*, 779; f) Newkome, G.

- R.; Moorefield, C. N. *Chem. Soc. Rev.* **2015**, *44*, 3954. Examples: g) Howlader, P.; Das, P.; Zangrando, E.; Mukherjee, P. S. *J. Am. Chem. Soc.* **2016**, *138*, 1668; h) Metherell, A. J.; Ward, M. D. *Chem. Sci.* **2016**, *7*, 910; i) Ronson, T. K.; Roberts, D. A.; Black, S. P.; Nitschke, J. R. *J. Am. Chem. Soc.* **2015**, *137*, 14502; j) Zhang, L.; Lin, Y.-J.; Li, Z.-H.; Jin, G.-X. *J. Am. Chem. Soc.* **2015**, *137*, 13670; k) Lee, H.; Noh, T. H.; Jung, O.-S. *Angew. Chem. Int. Ed.* **2016**, *55*, 1005; l) Chepelin, O.; Ujma, J.; Barran, P. E.; Lusby, P. J. *Angew. Chem. Int. Ed.* **2012**, *51*, 4194; m) Yamanaka, M.; Yamada, Y.; Sei, Y.; Yamaguchi, K.; Kobayashi, K. *J. Am. Chem. Soc.* **2006**, *128*, 1531; n) Zheng, Y.-R.; Zhao, Z.; Wang, M.; Ghosh, K.; Pollock, J. B.; Cook, T. R.; Stang, P. J. *J. Am. Chem. Soc.* **2010**, *132*, 16873; o) Schmidtdorf, M.; Pape, T.; Hahn, F. E. *Angew. Chem. Int. Ed.* **2012**, *51*, 2195; p) Prusty, S.; Krishnaswamy, S.; Bandi, S.; Chandrika, B.; Luo, J.; McIndoe, J. S.; Hanan, G. S.; Chand, D. K. *Chem. Eur. J.* **2015**, *21*, 15174; q) García-Simón, C.; Gramage-Doria, R.; Raoufmoghaddam, S.; Parella, T.; Costas, M.; Ribas, X.; Reek, J. N. H. *J. Am. Chem. Soc.* **2015**, *137*, 2680; r) Yoshizawa, M.; Nagao, M.; Kumazawa, K.; Fujita, M. *J. Organomet. Chem.* **2005**, *690*, 5383; s) Schmittel, M.; Ganz, A. *Chem. Commun.* **1997**, 999; t) Sun, Q.-F.; Sato, S.; Fujita, M. *Angew. Chem. Int. Ed.* **2014**, *53*, 13510.

8. a) Kishore, R. S. K.; Paululat, T.; Schmittel, M. *Chem. Eur. J.* **2006**, *12*, 8136; b) Schmittel, M.; Kalsani, V.; Michel, C.; Mal, P.; Ammon, H.; Jäckel, F.; Rabe, J. P. *Chem. Eur. J.* **2007**, *13*, 6223; c) Osuga, T.; Murase, T.; Fujita, M. *Angew. Chem. Int. Ed.* **2012**, *51*, 12199; d) Yan, X.; Cook, T. R.; Wang, P.; Huang, F.; Stang, P. J. *Nat Chem* **2015**, *7*, 342; e) Samanta, D.; Shanmugaraju, S.; Joshi, S. A.; Patil, Y. P.; Nethaji, M.; Mukherjee, P. S. *Chem. Commun.* **2012**, *48*, 2298; f) Samanta, D.; Mukherjee, P. S. *Chem. Commun.* **2014**, *50*, 1595; g) Cook, T. R.; Vajpayee, V.; Lee, M. H.; Stang, P. J.; Chi, K.-W. *Acc. Chem. Res.* **2013**, *46*, 2464.

9. a) Han, M.; Engelhard, D. M.; Clever, G. H. *Chem. Soc. Rev.* **2014**, *43*, 1848; b) Custelcean, R. *Chem. Soc. Rev.* **2014**, *43*, 1813; c) Frank, M.; Johnstone, M. D.; Clever, G. H. *Chem. Eur. J.* **2016**, *22*, 14104.

10. a) Johnstone, M. D.; Schwarze, E. K.; Ahrens, J.; Schwarzer, D.; Holstein, J. J.; Dittrich, B.; Pfeffer, F. M.; Clever, G. H. *Chem. Eur. J.* **2016**, *22*, 10791; b) Löffler, S.; Lübber, J.; Wuttke, A.; Mata, R. A.; John, M.; Dittrich, B.; Clever, G. H. *Chem. Sci.* **2016**, *7*, 4676; c) Zhou, L.-P.; Sun, Q.-F. *Chem. Commun.* **2015**, *51*, 16767; d) Kishi, N.; Li, Z.; Yoza, K.; Akita, M.; Yoshizawa, M. *J. Am. Chem. Soc.* **2011**, *133*, 11438; e) Liao, P.; Langloss, B. W.; Johnson, A. M.; Knudsen, E. R.; Tham, F. S.; Julian, R. R.; Hooley, R. J. *Chem. Commun.* **2010**, *46*, 4932.

11. a) Han, M.; Michel, R.; He, B.; Chen, Y.-S.; Stalke, D.; John, M.; Clever, G. H. *Angew. Chem. Int. Ed.* **2013**, *52*, 1319; b) Löffler, S.; Lübber, J.; Krause, L.; Stalke, D.; Dittrich, B.; Clever, G. H. *J. Am. Chem. Soc.* **2015**, *137*, 1060.

12. a) Zhu, R.; Lübber, J.; Dittrich, B.; Clever, G. H. *Angew. Chem. Int. Ed.* **2015**, *54*, 2796; b) Sekiya, R.; Fukuda, M.; Kuroda, R. *J. Am. Chem. Soc.* **2012**, *134*, 10987; c) Bandi, S.; Pal, A. K.; Hanan, G. S.; Chand, D. K. *Chem. Eur. J.* **2014**, *20*, 13122.

13. Frank, M.; Hey, J.; Balcioglu, I.; Chen, Y.-S.; Stalke, D.; Suenobu, T.; Fukuzumi, S.; Frauendorf, H.; Clever, G. H. *Angew. Chem. Int. Ed.* **2013**, *52*, 10102.

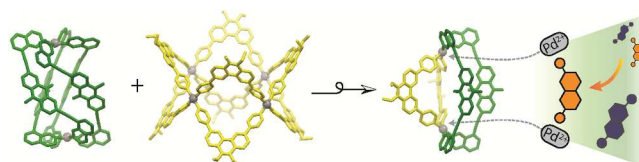
14. a) McNeill, S. M.; Preston, D.; Lewis, J. E. M.; Robert, A.; Knerr-Rupp, K.; Graham, D. O.; Wright, J. R.; Giles, G. I.; Crowley, J. D. *Dalton Trans.* **2015**, *44*, 1129; b) Ahmedova, A.; Momekova, D.; Yamashina, M.; Shestakova, P.; Momekov, G.; Akita, M.; Yoshizawa, M. *Chem. Asian J.* **2016**, *11*, 474.

15. a) Safont-Sempere, M. M.; Fernández, G.; Würthner, F. *Chem. Rev.* **2011**, *111*, 5784; b) Lal Saha, M.; Schmittel, M. *Org. Biomol. Chem.* **2012**, *10*, 4651; c) Jiménez, A.; Bilbeisi, R. A.; Ronson, T. K.; Zarra, S.; Woodhead, C.; Nitschke, J. R. *Angew. Chem. Int. Ed.* **2014**, *53*, 4556; d) Yan, L.-L.; Tan, C.-H.; Zhang, G.-L.; Zhou, L.-P.; Bünzli, J.-C.; Sun, Q.-F. *J. Am. Chem. Soc.* **2015**,

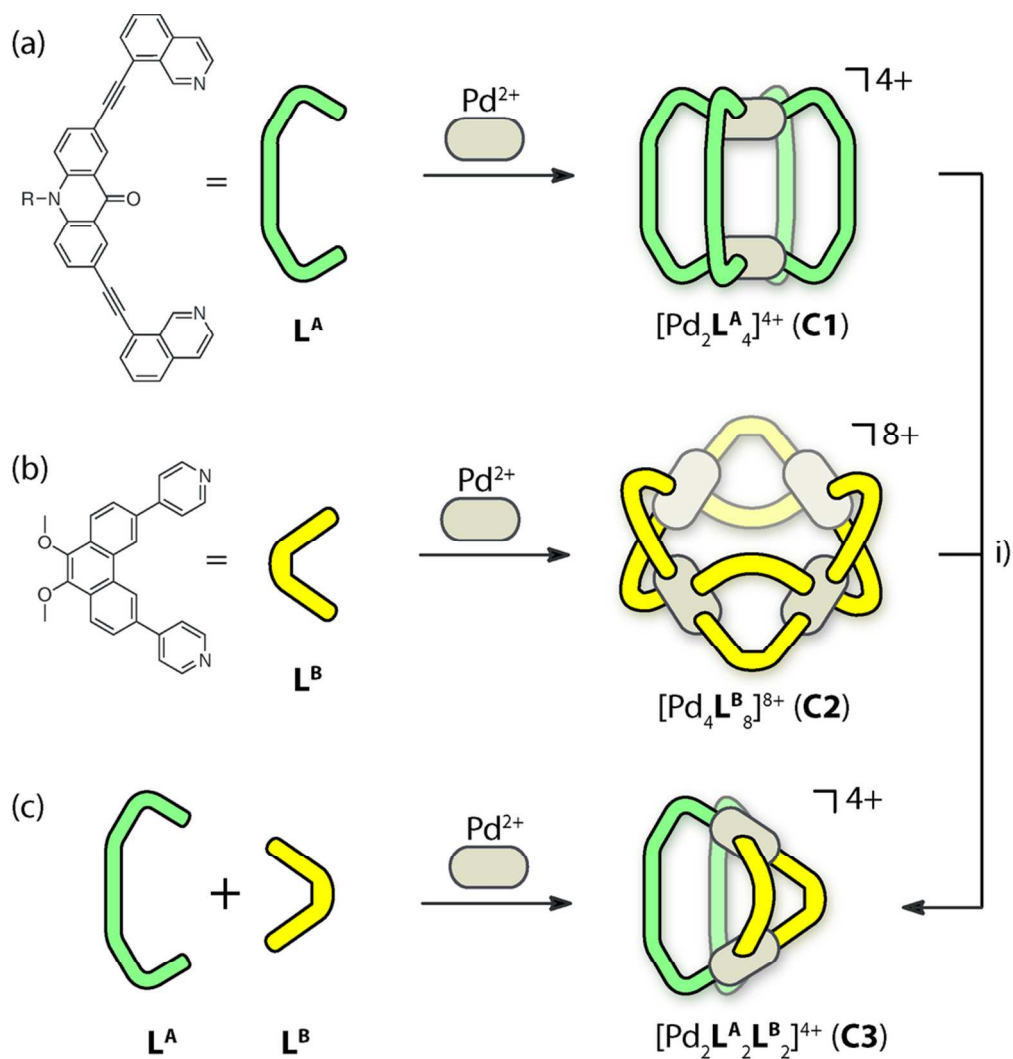
1 137, 8550; e) Johnson, A. M.; Wiley, C. A.; Young, M. C.; Zhang,
2 X.; Lyon, Y.; Julian, R. R.; Hooley, R. J. *Angew. Chem.* **2015**, *127*,
3 5733.
4 16. a) Frank, M.; Ahrens, J.; Bejenke, I.; Krick, M.; Schwarzer,
5 D.; Clever, G. H. *J. Am. Chem. Soc.* **2016**, *138*, 8279; b) Frank, M.;
6 Krause, L.; Herbst-Irmer, R.; Stalke, D.; Clever, G. H. *Dalton*
7 *Trans.* **2014**, *43*, 4587.
8 17. Johnson, A. M.; Hooley, R. J. *Inorg. Chem.* **2011**, *50*, 4671.
9 18. Yamashina, M.; Yuki, T.; Sei, Y.; Akita, M.; Yoshizawa, M.
10 *Chem. Eur. J.* **2015**, *21*, 4200.
11 19. Preston, D.; Barnsley, J. E.; Gordon, K. C.; Crowley, J. D. *J.*
12 *Am. Chem. Soc.* **2016**, *138*, 10578.
13 20. a) Stang, P. J.; Olenyuk, B. *Acc. Chem. Res.* **1997**, *30*, 502; b)
14 Fujita, M.; Fujita, N.; Ogura, K.; Yamaguchi, K. *Nature* **1999**, *400*,

52; c) Klotzbach, S.; Beuerle, F. *Angew. Chem. Int. Ed.* **2015**, *54*,
10356.
21. a) Suzuki, K.; Kawano, M.; Fujita, M. *Angew. Chem.* **2007**,
119, 2877; b) Kumar Chand, D.; Fujita, M.; Biradha, K.; Sakamoto,
S.; Yamaguchi, K. *Dalton Trans.* **2003**, 2750.
22. Wang, W.; Wang, Y.-X.; Yang, H.-B. *Chem. Soc. Rev.* **2016**,
45, 2656.
23. Clever, G. H.; Tashiro, S.; Shionoya, M. *Angew. Chem. Int.*
Ed. **2009**, *48*, 7010; b) Clever, G. H.; Kawamura, W.; Shionoya, M.
Inorg. Chem. **2011**, *50*, 4689.

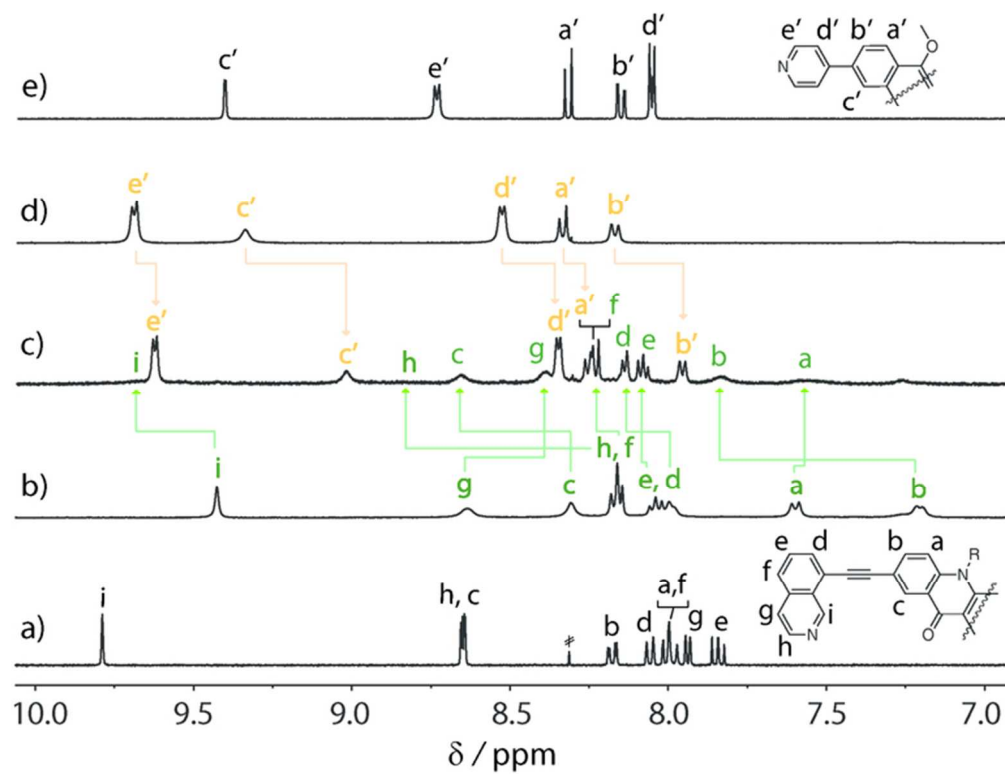
Table of Contents artwork

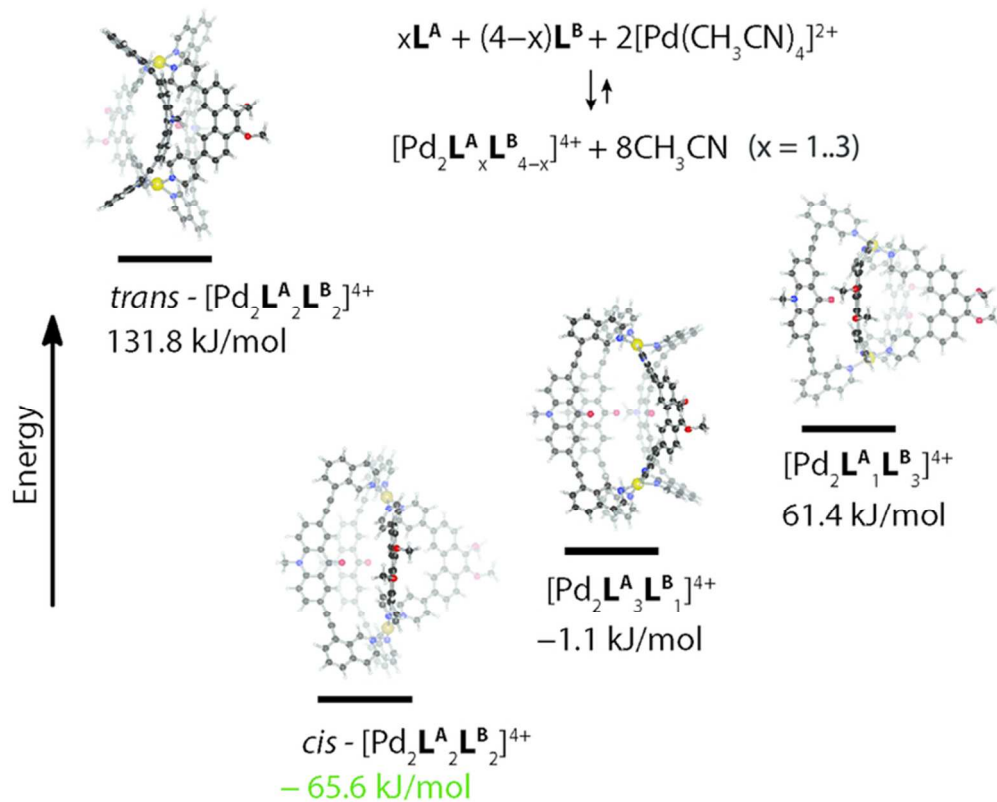


1
2
3
4
5
6
7
8
9
10
11
12
13
14
15
16
17
18
19
20
21
22
23
24
25
26
27
28
29
30
31
32
33
34
35
36
37
38
39
40
41
42
43
44
45
46
47
48
49
50
51
52
53
54
55
56
57
58
59
60

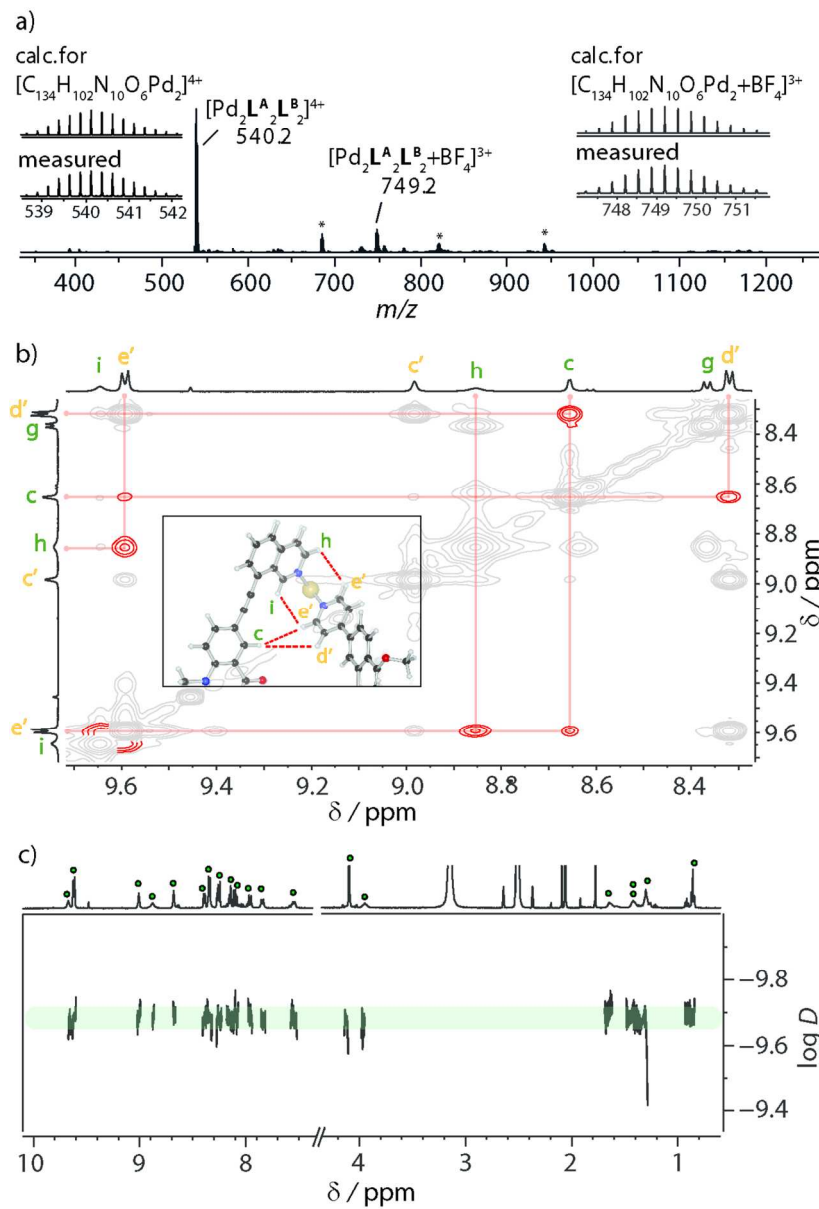


87x92mm (300 x 300 DPI)

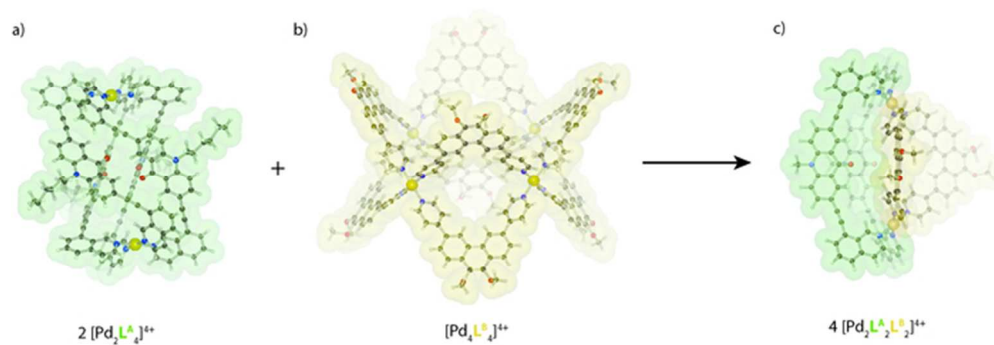




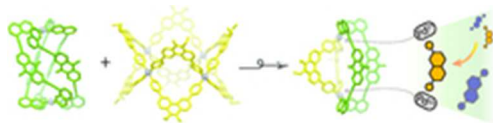
68x55mm (300 x 300 DPI)



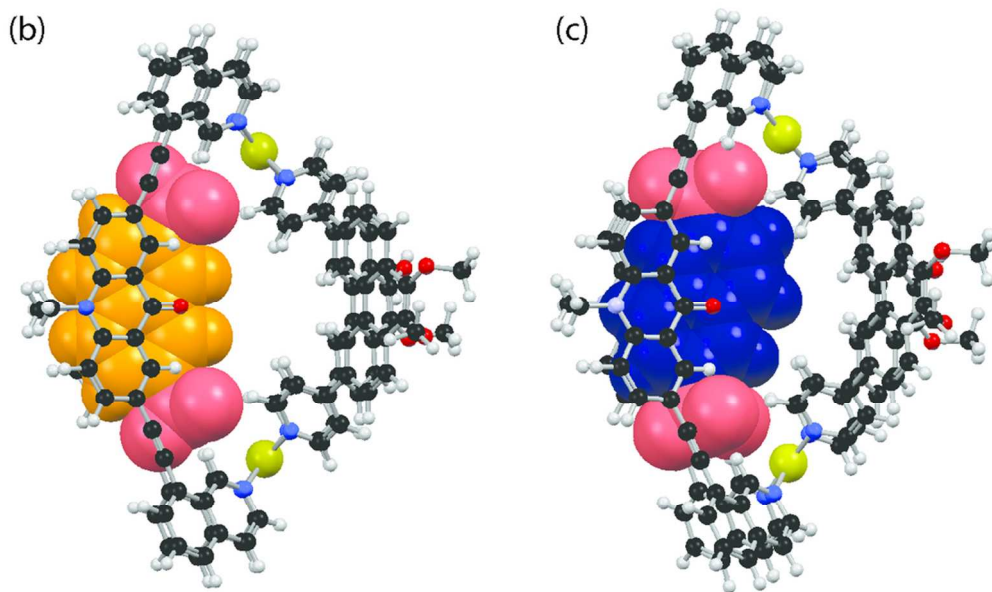
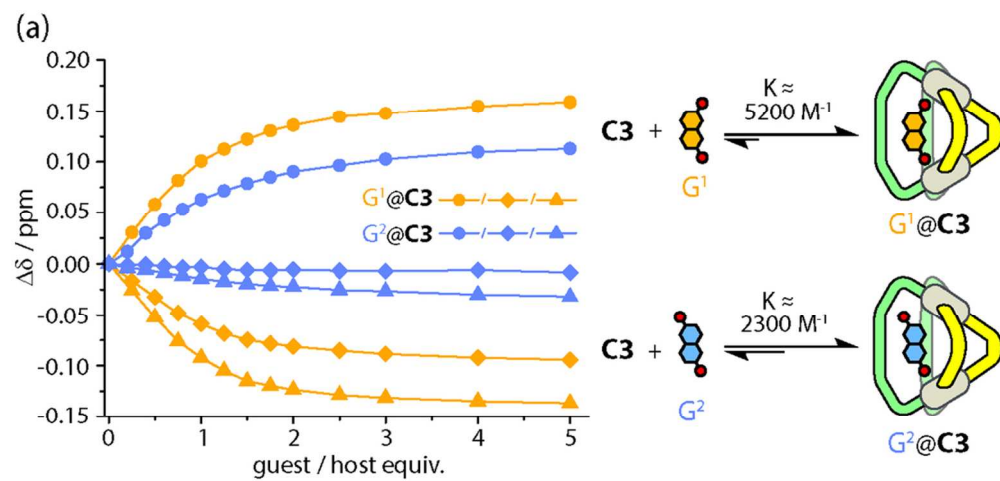
124x183mm (300 x 300 DPI)



59x21mm (300 x 300 DPI)



20x5mm (300 x 300 DPI)



93x104mm (300 x 300 DPI)